Design and implementation of finite-time control for speed tracking of permanent magnet synchronous motors

Chakib Chatri, Moussa Labbadi, Mohammed Ouassaid, Kamal Elyaalaoui, Yassine El

Design and implementation of finite-time control for speed tracking of permanent magnet synchronous motors

Chakib Chatri, Moussa Labbadi, Mohammed Ouassaid, Kamal Elyaalaoui and Yassine El Houm

***Abstract*— This letter investigates real-time implementation of a finite-time control for permanent magnet synchronous motors in the presence of external load disturbance. Firstly, an integral terminal sliding manifold is designed to achieve fast speed, high precision performance, and to enhance the quality of currents by reducing the total harmonic distortion. Indeed, the proposed surface manifold ensures a finite-time convergence of the speed state variable. Secondly, a switching control scheme is added for the system control to force the state systems to converge to their desired values in the presence of load disturbance. Finite-time stability is proved based on Lyapunov theory. Finally, the effectiveness of the designed controller is validated by carrying out real-time experimental studies using eZdspTM F28335 board. According to the experimental results, the proposed controller is easy to implement, improves tracking accuracy, reduces the chattering issues and ensures robustness against external load disturbance.**

***Index Terms*— Permanent magnet synchronous motor, integral terminal sliding mode control, finite-time control.**

I. Introduction

Currently, with the rapid progress of digital signal processors (DSP) and power electronics tools, the permanent magnet synchronous motor (PMSM) is considered one of the preferred alternating current (AC) motors used in various fields, e.g., electric vehicles, aerospace drives, robotics, medical equipment, etc. Compared to other AC motors, the PMSM has excellent performance, such as a high torque/inertia ratio, high power density, lightweight, and lower maintenance requirements. However, the effectiveness of speed regulation of PMSM is typically dependent on nonlinear servo with complex states, time-variation, and parametric uncertainties [1]. In this situation, a classical linear control strategy might not guarantee high tracking performance for a PMSM-based nonlinear system.

To overcome all these disadvantages and enhance tracking performance, several control strategies have been investigated. These strategies come in two main categories: intelligent and nonlinear controls. First, intelligent control techniques have been adopted to approximate non-linearity [2]. Nevertheless, the design of intelligent controllers involves complex calculation efforts due to training conditions and sophisticated algorithms. On the other hand, many nonlinear controllers have been developed for the aforementioned issues, such as nonlinear proportional-integral (PI) control [3], backstepping control [4], sliding mode control (SMC) [5], etc. Among these nonlinear control techniques, SMC is one of the popular strategies for nonlinear systems, because of its fast dynamics and excellent level of robustness against uncertainties [5]. SMC was implemented for the speed motor of the PMSM to enhance the speed tracking precision. But, the use of a large switching gain to ignore disturbances like varying load torque significantly increases the chattering, degrading the speed tracking performance. The chattering phenomenon and the state variables of PMSM also require infinite time to converge to the origin. These are the main drawbacks of the classical SMC, which are not desirable in real applications [6]. To address these issues in SMC, a terminal sliding mode control (TSMC) has been developed for PMSM drive systems [7], [8]. For example, in [9], TSMC through feedback linearization technique was proposed to control the speed/current of PMSM. However, only numerical results were presented due to the complexity of the controller. Similarly, [10] presented an event-triggered TSMC to regulate the speed of the PMSM with the primary goal of improving speed control performance and reducing chattering. In [11], an action integral was added to TSMC to enhance the dynamic performance of speed tracking under torque ripple and external disturbance. Paper [12] proposed a second-order TSMC to obtain a fast convergence and reduce the chattering phenomena.

Motivated by the previous studies, a nonlinear controller is designed for the PMSM servo. Firstly, an integral sliding manifold is proposed to converge in a finite time and enhance the tracking performance of the state variables of the PMSM. Secondly, a reaching control law is added to reinforce the robustness against load disturbance. Thirdly, the Lyapunov stability theory is used to verify integral terminal sliding mode control (ITSMC) stability to implement it in real-time applications. Accordingly, the main highlights and contributions of this letter are as follows:

- The proposed control scheme ensures finite-time convergence of motor speed by utilizing an integral sliding manifold.
- An ITSMC controller is designed for the PMSM, which is characterized by faster tracking, higher robustness against perturbation, and lower chattering phenomenon.
- Three cases are taken into account to verify the performance of the suggested controller: constant speed, steep

C. Chatri, M. Ouassaid and Y. El Houm are with Engineering for Smart and Sustainable Systems Research Center, Mohammadia School of Engineers, Mohammed V University in Rabat, Morocco.(e-mail: chakibchatri@research.emi.ac.ma; ouassaid@emi.ac.ma; yassineelhoum@research.emi.ac.ma).

M. Labbadi is with the Univ. Grenoble Alpes, CNRS, Grenoble INP, GIPSA-lab, 38000 Grenoble, France. (e-mail: moussa.labbadi@gipsa-lab.grenoble-inp.fr).

K. Elyaalaoui is with the LAPLACE, University of Toulouse, INPT, France.(e-mail: kamalelyaalaoui@research.emi.ac.ma).

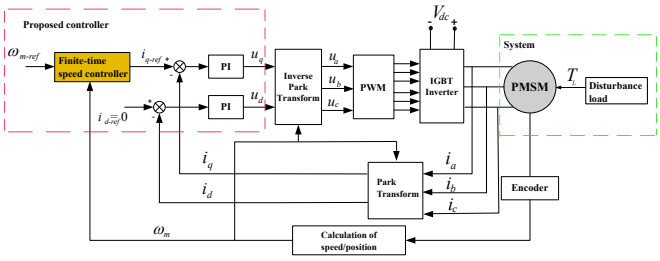

Fig. 1. An overall schematic of the proposed control for the PMSM.

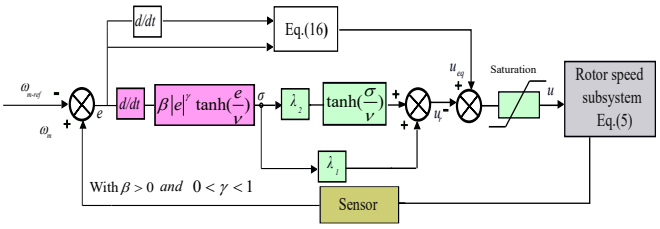

Fig. 2. Block diagram of the adopted ITSMC.

speed, and external load disturbance.

- Real-time experimentation is carried out to validate the efficiency of the proposed controller.

The outline of the present letter is as follows. Section II briefly introduces the problem formulation of PMSM control. Section III provides the proposed controller based on ITSMC. Section IV presents the experimental results with different scenarios to verify the effectiveness of the proposed strategy. The conclusion part of this paper is given in Section V.

II. Problem Formulation

A schematic of the proposed controller for the PMSM is illustrated in Fig. 1. The control system includes two main loops: the outer loop is reserved for regulation of the motor speed, while the inner loop is applied to adjust the stator currents at their reference values. The speed value measured by the encoder is compared to its reference value, and then the error is sent to the outer-loop that generates the current reference i_{q-ref} and tracks the desired speed in a finite time. Using the vector control method $i_{d-ref} = 0$, the motor speed and stator currents are decoupled. The current errors are applied to the input of the PI regulators in order to stabilize the currents and generate the control inputs u_d and u_q. Therefore, the design of an ITSMC-based speed controller is the major contribution of the present letter. The dynamic current of the PMSM in the d-q coordinates is expressed as follows [4]:

$$\begin{cases} \dfrac{di_d}{dt} = -\dfrac{R_m}{L_d} i_d + \dfrac{L_q}{L_d} p_m \omega_m i_q + \dfrac{1}{L_d} u_d \\ \dfrac{di_q}{dt} = -\dfrac{R_m}{L_q} i_{sq} - \dfrac{L_d}{L_q} p_m \omega_m i_d - \dfrac{p_m \omega_m}{L_q} \Psi_{mf} + \dfrac{1}{L_q} u_q \end{cases} \tag{1}$$

where R_m, p_m, ω_m, and Ψ_{mf} represent the motor resistance, number of pole pairs, motor speed, and flux linkage of permanent magnet, respectively; L_d and L_q denote the dq axis inductance stator; u_d and u_q denote stator voltages in d-q farm.

The motion equation of the PMSM is described as follows:

$$\frac{d\omega_m}{dt} = \frac{1}{J_m}(T_{em} - B_m \omega_m - T_L) \tag{2}$$

where J_m, B_m, and T_L represent the motor inertia, the viscous friction coefficient, and the load torque, respectively. T_{em} denotes the electromagnetic torque developed by PMSM, which can be expressed by:

$$T_{em} = \frac{3p_m}{2}\left(\Psi_{mf} i_q + (L_d - L_q) i_d i_q\right) \tag{3}$$

For surface mounted PMSM, the inductance in d axis equals that in q axis, i.e. $L_d = L_q$, the electromagnetic torque is simplified as follows:

$$T_{em} = \frac{3p_m \Psi_{mf}}{2} i_q \tag{4}$$

Using (4), the state space equation (2) can be rewritten as follows:

$$\dot{x} = f(x) + gu + d \tag{5}$$

where $x = \omega_m$, $f(x) = \dfrac{-B_m}{J_m}\omega_m$, $u = i_q$, $g = \dfrac{3p_m \Psi_{mf}}{2J_m}$, and $d = \dfrac{-T_L}{J_m}$ (with T_L an unknown disturbance).

III. Main Results

In this section, a controller based on ITSMC is proposed to stabilize the tracking speed of PMSM. The expression of ITSM manifolds can be defined as:

$$\sigma = e + \xi \int_0^t h(e(\tau))d\tau \quad \xi > 0 \tag{6}$$

where $h(e(\tau))$ is a switching function (refer to [13]) described as:

$$h(e(\tau)) = sign(e(\tau)) \tag{7}$$

The integration of $sign(e(\tau))$ ensures fast convergence of tracking error when it is far from the equilibrium point but $sign(e(\tau))$ provides higher chattering in control law.

The authors of [14] proposed a terminal attractor as described by the following equation:

$$h(e(\tau)) = e(\tau)^{p/q} \quad 0 < p/q < 1 \tag{8}$$

The integral term of $e(\tau)^{p/q}$ achieves a finite-time convergence of the speed state variable, but it is still not as robust as (7) when the tracking error is far from the equilibrium point, due to the lack of a switching function. The main contribution of this letter is to design an ITSMC based on switching function, as shown in Fig. 2. The performances of both (7) and (8) are combined to assure that the state variables converge to zero in finite time. The performance of the proposed method and two ITSMC approaches are compared using simulation results, as shown in Fig.3.

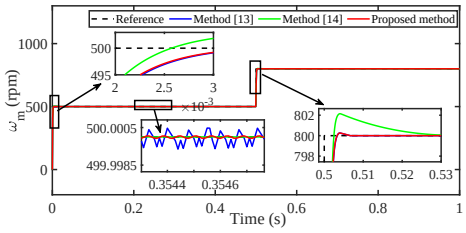

Fig. 3. Performance comparison of three controllers.

The proposed controller is designed by the following steps below.

The speed tracking error is defined as:

$$e(t) = x - x_{ref} \tag{9}$$

where $x_{ref} = \omega_{m-ref}$ is the speed reference of the motor.

The integral terminal sliding surface is given by:

$$\sigma(t) = e(t) + \beta \int sig^{\gamma}\big(e(t)\big)dt \tag{10}$$

here $sig\big(e(t)\big) = |e(t)|^{\gamma} sign\big(e(t)\big)$, $\beta > 0$, and $0 < \gamma < 1$. Note that

$$\dot{e}_I(t) = sig^{\gamma}(e(t)) \tag{11}$$

On the surface $\sigma(t) = 0$ i.e., $\big(e(t) = -\beta e_I(t)\big)$, the integrator (11) yields:

$$\dot{e}_I(t) = -\beta^{\gamma} sig^{\gamma}\big(e_I(t)\big) \tag{12}$$

From solving (12), the convergent time of $e_I(t)$ is:

$$\tau_s = \frac{|e_I(0)|^{(1-\gamma)}}{\beta^{\gamma}(1-\gamma)} = \frac{|e(0)|^{(1-\gamma)}}{\beta(1-\gamma)} \tag{13}$$

Meanwhile, the settling time for the convergence of the tracking error $e(t)$ is also τ_s.

The derivative of (10) gives:

$$\dot{\sigma}(t) = \dot{e}(t) + \beta|e(t)|^{\gamma} sign\big(e(t)\big) \tag{14}$$

According to (5) and (9), the time derivative $\dot{\sigma}(t)$ yields:

$$\dot{\sigma}(t) = f(x) + gu + d - \dot{x}_{ref} + \beta|e(t)|^{\gamma} sign\big(e(t)\big) \tag{15}$$

Supposing that $d = 0$, then the equivalent control law is:

$$u_{eq} = \frac{1}{g}\left[-f(x) + \dot{x}_{ref} - \beta|e(t)|^{\gamma} sign\big(e(t)\big)\right] \tag{16}$$

To increase the performance tracking of speed regulation, the switching control law u_r is added to the equivalent control law as follows:

$$\begin{cases} u = u_{eq} + u_r \\ u_r = \dfrac{1}{g}\Big[-\lambda_1\sigma(t) - (\lambda_2 + \eta)sign(\sigma(t))\Big] \end{cases} \tag{17}$$

where $\lambda_1 > 0$, $\lambda_2 > |d| > 0$, and η is a small parameter to be designed. Then, the virtual control of the speed motor loop is given as:

$$\begin{aligned} u = \frac{1}{g}\Big[&-f(x) + \dot{x}_{ref} - \beta|e(t)|^{\gamma} sign(e(t)) \\ &- \lambda_1\sigma(t) - (\lambda_2 + \eta)sign(\sigma(t))\Big] \end{aligned} \tag{18}$$

The control law presented in (18) is implemented assuming that the following condition is satisfied $d < |d| < \lambda_2$. The proposed controller has the following characteristics: (i) the finite convergence time can be adapted in accordance with (13); (ii) combines the terminal attractor and switching function to get a fast convergence of tracking error when it is far from the equilibrium point; (iii) switching control law is added to strengthen the robustness against load disturbance.

A. Stability analysis

The main results of the paper are given in the following theorem and the stability is ensured. If $\lambda_2 > |d|$, the closed-loop motor speed subsystem (5), tracking error (9), integral terminal sliding mode surface (10) and controller (18) is finite-time stable. Then, the global convergence asymptotic of speed tracking error to zero in finite-time is achieved and the settling time is $\tau = \tau_p + \tau_s$. *Proof:* Define the Lyapunov function as:

$$\vartheta(t) = \frac{1}{2}\sigma(t)^2 \tag{19}$$

Differentiating $\vartheta(t)$ with respect to time gives:

$$\dot{\vartheta}(t) = \sigma(t)\dot{\sigma}(t) \tag{20}$$

Upon substituting (15) into (20), then $\dot{\vartheta}(t)$ becomes:

$$\dot{\vartheta}(t) = \sigma(t)\Big[f(x) + gu + d - \dot{x}_{ref} + \beta|e(t)|^{\gamma} sign(e(t))\Big] \tag{21}$$

According to the control law designed in (18) and after a simple calculation, equation (21) becomes:

$$\dot{\vartheta}(t) = -\lambda_1\sigma(t)^2 + d - (\lambda_2 + \eta)\sigma(t)sign(\sigma(t)) \tag{22}$$

Thus:

$$\dot{\vartheta}(t) \le -\lambda_1\sigma(t)^2 - \eta\,|\sigma(t)| < 0 \tag{23}$$

Consequently, ϑ (assuming $\forall\, t \ge \tau_{p0}, \vartheta\,(\tau_{p0}) \ge 0$ where τ_{p0} denotes the initial time) converges to zero in a finite time τ_p. To determinate τ_p and complete the proof of the theorem, the $\dot{\vartheta}(t)$ can be rewritten as follows:

$$\frac{d\vartheta}{dt} \le -2\lambda_1\vartheta - 2^{1/2}\eta\vartheta^{1/2} \tag{24}$$

Dividing (24) by $\vartheta^{1/2}$, it results in:

$$dt \le \frac{-\vartheta^{-1/2}}{2\lambda_1\vartheta^{1/2} + \sqrt{2}\eta}d\vartheta \tag{25}$$

By integrating (25) from τ_{p0} to τ_p, the time τ_p is calculated as follows:

$$\begin{aligned} \tau_p - \tau_{p0} &\le -\int_{\vartheta(\tau_{p0})}^{0} \frac{\vartheta^{-1/2}}{2\lambda_1\vartheta^{0.5} + \sqrt{2}\eta}d\vartheta \\ &= \frac{1}{\lambda_1}\ln\frac{2\lambda_1\vartheta^{0.5}\,(\tau_{p0}) + \sqrt{2}\eta}{\sqrt{2}\eta} \end{aligned} \tag{26}$$

Thus, from the analysis above, the motor speed loop converges to zero in finite time τ, which is defined as follows:

$$\tau = \tau_p + \tau_s \tag{27}$$

TABLE I
PMSM PARAMETERS.

Parameter	Value
P_{rated}	rated power : $400(w)$
V_{dc}	DC voltage : $48(V)$
T_{em}	rated rated torque : $1.27(N.m)$
R_m	motor resistance :$3.25(\Omega)$
$L_d = L_q$	motor inductance :$0.007(H)$
J_m	motor inertia : $3.1e^{-5}(Kg.m^2)$
B_m	friction coefficient :$4e^{-6}(Nm.s/rad)$
Ψ_{mf}	flux linkage : $0.0436(wb)$
p_m	pole pairs : 4

with τ_s given in (13). Hence, the finite-time convergence of the speed tracking error is obtained. ■

Fig. 4 illustrates the flowchart of the proposed ITSMC to drive the PMSM. As shown in Fig. 4, the proposed ITSMC (18) is designed to track the speed reference, and the q-axis reference current (i_{q-ref}) is generated by the output of the speed control loop. In order to reduce the chattering issue, the discontinuous control component $sign(.)$ function, in the control laws of SMC and proposed ITSMC, is replaced by the $\tanh(./\nu)$ function, where ν is a small positive parameter. The value of ν is adjusted to 0.05, which is the value selected to achieve the best balance between tracking accuracy and control smoothness.

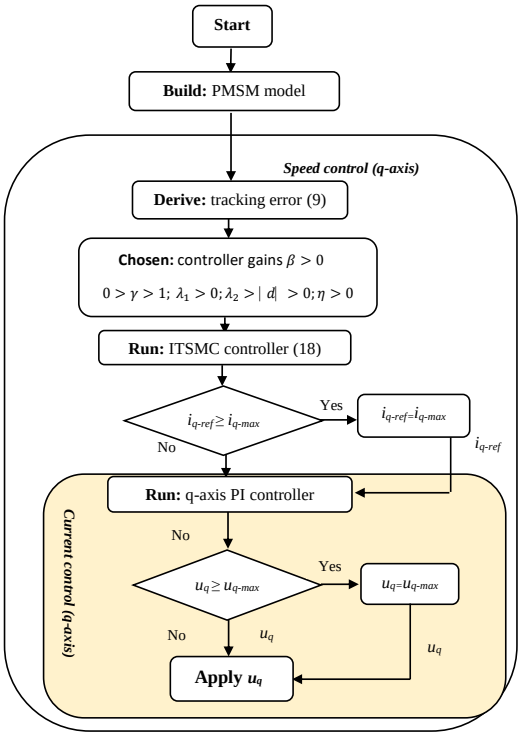

Fig. 4. Flowchart of the proposed ITSMC to drive the PMSM.

IV. EXPERIMENTAL VALIDATION

This section presents experimental results as a means to validate the effectiveness of the proposed controller scheme. The laboratory experimental test bench is displayed in Fig. 5(a) and its configuration is shown in Fig. 5(b). The test bench comprises PMSM, a direct-current (DC) generator, a power inverter, a computer, a DSP board, a power analyzer, a multimeter, an incremental encoder and a DC load. The machine parameters are given in Table I. To evaluate the performance of the proposed controller, three different cases are considered, e.g., constant speed, steep speed, and external load disturbance. In all studied cases, the ITSMC parameters are assumed as follows: $\beta = 3.25$, $\gamma = 0.6$, $\lambda_1 = 32$, and $\lambda_2 = 32$.

A. Constant speed

Fig. 6 shows the experimental results of the motor speed ω_m, the direct current i_d, and the quadrature i_q current using the SMC (Blue) and the proposed controller (Red). As shown in Fig. 6(a), the motor speed perfectly tracks the constant reference (700 rpm) using the proposed controller, while the SMC cannot satisfy the tracking performance. As it can be seen from Figs. 6(b) and 6(c), the ripples of the direct current and quadrature current are considerably attenuated using the proposed controller instead of the conventional SMC.

To confirm the efficiency and the high performance of the proposed control, the current harmonics are carried out through the power analyzer, as shown in Fig. 7. The two results are compared side-by-side to demonstrate the superiority of the proposed controller in terms of power quality improvement and reduction of the current total harmonic distortion (THD). The maximum values of the THD current are reduced from [4.1%, 5%, 4.3%], using the conventional SMC, to reach the lower values of [2.4%, 3.2%, 2.5%] using the proposed controller. Therefore, it can be concluded that the proposed ITSMC technique is developed to overcome the problem of the chattering effect, which generates higher THD at the inverter output during the SMC operation.

B. Steep change speed

To study the dynamic response and the transient behavior of the PMSM under SMC and ITSMC methods, a steep change of the rotor speed is applied, as shown in Fig. 8(a). The fast increase of the rotational reference speed from 300 rpm to 900 rpm led to a fast increase of the quadrature current i_q (see Fig. 8(b)), while the direct current remains constant (see Fig.8(c)), which demonstrates that the direct current and quadrature current are perfectly decoupled. Fig. 8(a) shows that fast response and high-performance acceleration are obtained using the proposed speed controller compared to the response given by the conventional SMC. In addition, the settling times of the speed responses under SMC and ITSMC are $1.22s$ and $0.3s$, respectively. According to Fig. 8(b) and Fig. 8(c), the current ripple and chattering of i_q and i_d under ITSMC are significantly reduced.

In this scenario, the experimental results confirm the good dynamic response of the proposed method despite the speed variation.

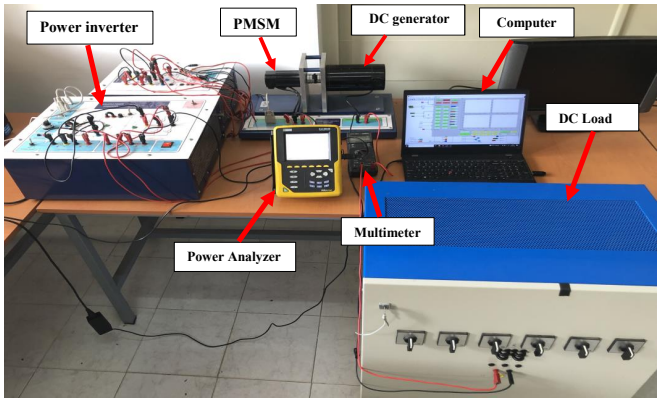

(a)

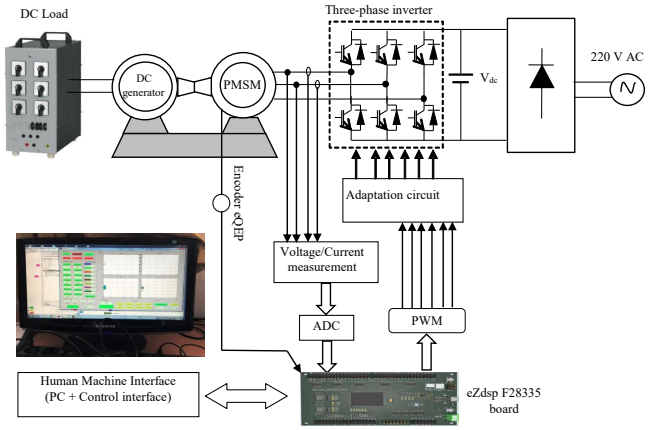

(b)

Fig. 5. Experimental implementation: (a) laboratory experimental test bench, (b) configuration of the experimental test setup.

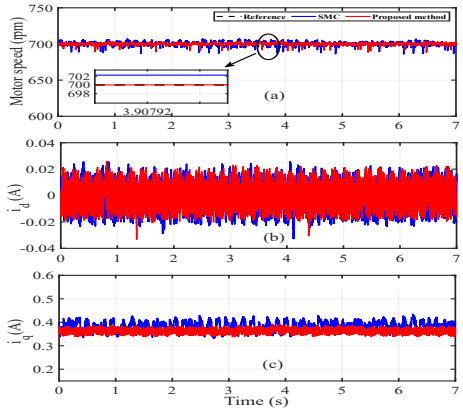

Fig. 6. Experimental results of the state variables of the PMSM when the reference speed equals 700 rpm: (a) motor speed, (b) direct current, (c) quadrature current.

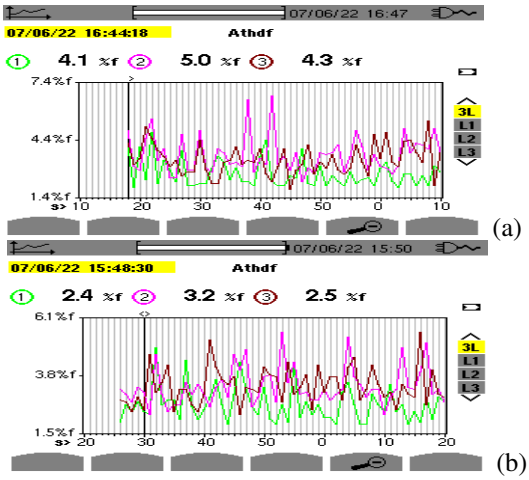

Fig. 7. Experimental results of the current THD: a) experimental results using SMC, b) experimental results using proposed method.

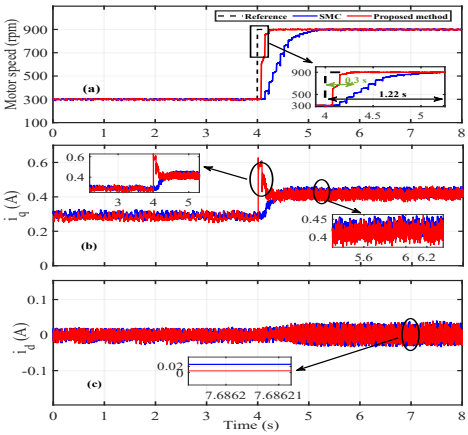

Fig. 8. Experimental results of the state variables of the PMSM under steep change speed: (a) motor speed, (b) quadrature current, (c) direct current.

C. External load variation

In the third scenario, an external load is added at the terminal of a DC generator to compare the robustness of the SMC and the proposed method. Fig. 9 shows the responses under a 50 % load disturbance at 700 rpm. According to Fig. 9(a), when 50% of load disturbance is added at $t = 4s$ on the PMSM system, the dynamic motor speed response under SMC fluctuates more than ITSMC. It is easily observed that the recovery times to reference speed under ITSMC and SMC are $T_1 = 0.15s$ and $T_2 = 0.75s$, respectively. The quadrature current and direct current are perfectly decoupled despite the added load, as shown in Figs 9(b) and 9(c). Besides, the response of the quadrature current i_q under ITSMC has faster convergence and less chattering compared to SMC. To further demonstrate the robustness of the proposed method and SMC, a larger load is added and removed. The speed curves based on SMC and ITSMC are illustrated in Figs. 10 and 11, respectively. When the load disturbance is added, it can be seen from Figs 10(b) and 11(b) that the speed drops under SMC and ITSMC are 117

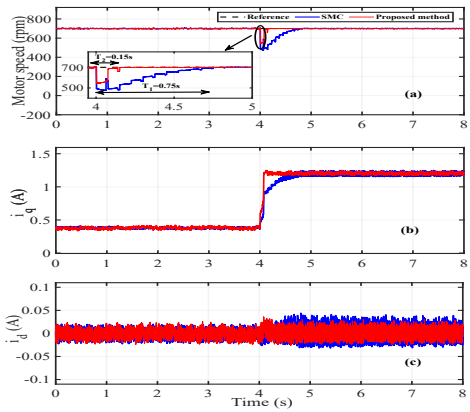

Fig. 9. Experimental results under 50 % load disturbance at 700 rpm: (a) motor speed, (b) quadrature current, (c) direct current.

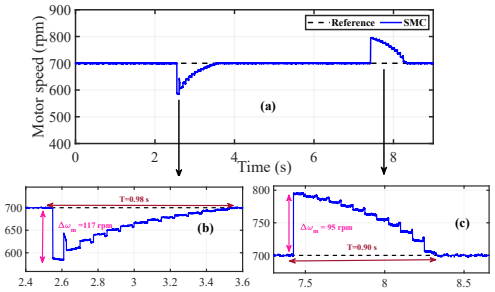

Fig. 10. Experimental results under SMC in the presence of external load disturbance at 700 rpm: (a) motor speed, (b) zoom when the load disturbance is added, (c) zoom when the load disturbance is removed.

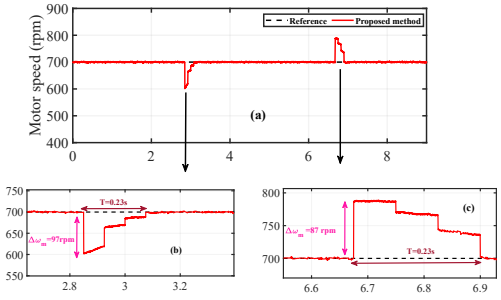

Fig. 11. Experimental results under ITSMC in the presence of external load disturbance at 700 rpm: (a) motor speed, (b) zoom when the load disturbance is added, (c) zoom when the load disturbance is removed.

rpm and 97 rpm, and the recovery times are $0.98s$ and $0.23s$, respectively. However, if the load disturbance is removed, it can be observed, from 10(c) and 11(c), that the overshoots at 700 rpm are 95 rpm and 87 rpm, and the recovery times to the reference speed are $0.90s$ and $0.23s$, respectively.

As a result, compared with SMC, the proposed controller has a faster recovery time and a smaller overshoot/drop under the load disturbance.

V. Conclusion

In this letter, a nonlinear ITSMC speed control technique has been developed to obtain fast speed tracking and enhance the quality of the current of the PMSM drive. The proposed control system has been implemented by using ZdspTM F28335. The stability analysis proved the convergence to zero of the speed error in the finite-time using ITSMC law. The experimental results for different scenarios demonstrate that the proposed controller provides quick and accurate speed tracking compared to the SMC.

Acknowledgment

The authors gratefully acknowledges the financial support from the ANR (French National Research Agency) through the project by FRANCE RELANCE Grenoble INP- SOBEN.

References

[1] A. Bosso, A. Tilli, and C. Conficoni, A Hybrid Sensorless Observer for the Robust Global Asymptotic Flux Reconstruction of Permanent Magnet Synchronous Machines, *IEEE Control Syst. Lett.*, vol. 6, pp. 11, 2022.

[2] A. Ghamri, R. Boumaaraf, M. T. Benchouia, H. Mesloub, A. Gola, and N. Gola, Comparative study of ANN DTC and conventional DTC controlled PMSM motor, *Math. Comput. Simul.*, vol. 167, pp. 219230, 2020.

[3] Y. W. Jeong and C. C. Chung, Nonlinear Proportional-Integral Disturbance Observers for Motion Control of Permanent Magnet Synchronous Motors, *IEEE Control Syst.* Lett., vol. 6, pp. 30623067, 2022.

[4] X. Sun, H. Yu, J. Yu, and X. Liu, Design and implementation of a novel adaptive backstepping control scheme for a PMSM with unknown load torque, *IET Electr. Power Appl.*, vol. 13, no. 4, pp. 445455, 2019.

[5] V. Repecho, A. Sierra-Gonzalez, E. Ibarra, D. Biel, and A. Arias, Enhanced DC-Link Voltage Utilization for Sliding-Mode-Controlled PMSM Drives, *IEEE J. Emerg. Sel. Top. Power Electron.*, vol. 9, no. 3, pp. 28502857, 2021.

[6] A. K. Junejo, W. Xu, C. Mu, M. M. Ismail, and Y. Liu, Adaptive Speed Control of PMSM Drive System Based a New Sliding-Mode Reaching Law, *IEEE Trans. Power Electron.*, vol. 35, no. 11, pp. 1211012121, 2020.

[7] H. Wang, S. Li, and Z. Zhao, Design and implementation of chattering free sliding mode control method for PMSM speed regulation system, Proc. IEEE Int. Conf. Ind. Technol., vol. 2015-June, no. June, pp. 20692074, 2015.

[8] W. Xu, Y. Jiang, and C. Mu, Nonsingular terminal sliding mode control for speed regulation of permanent magnet synchronous motor with parameter uncertainties and torque change, 2015 18th Int. Conf. Electr. Mach. Syst. ICEMS 2015, pp. 20342039, 2016, doi: 10.1109/ICEMS.2015.7385375.

[9] X. Liu, H. Yu, J. Yu, and L. Zhao, Combined Speed and Current Terminal Sliding Mode Control with Nonlinear Disturbance Observer for PMSM Drive, *IEEE Access*, vol. 6, pp. 2959429601, 2018.

[10] J. Song, Y. K. Wang, Y. Niu, H. K. Lam, S. He, and H. Liu, Periodic Event-Triggered Terminal Sliding Mode Speed Control for Networked PMSM System: A GA-Optimized Extended State Observer Approach, *IEEE/ASME Trans. Mechatronics*, 2022.

[11] T. Yang, Y. Deng, H. Li, Z. Sun, H. Cao, and Z. Wei, Fast integral terminal sliding mode control with a novel disturbance observer based on iterative learning for speed control of PMSM, ISA Trans., no. xxxx, 2022, doi: 10.1016/j.isatra.2022.07.029.

[12] E. Lu, W. Li, X. Yang, and Y. Liu, Anti-disturbance speed control of low-speed high-torque PMSM based on second-order non-singular terminal sliding mode load observer, ISA Trans., vol. 88, pp. 142152, 2019.

[13] C. S. Chiu, Derivative and integral terminal sliding mode control for a class of MIMO nonlinear systems, Automatica, vol. 48, no. 2, pp. 316326, 2012.

[14] C. Chatri, M. Ouassaid, M. Labbadi, and Y. Errami, Integral-type terminal sliding mode control approach for wind energy conversion system with uncertainties, *Comput. Electr. Eng.*, vol. 99, no. May 2021, p. 107775, 2022.